# Probing the 2,4-Dichlorophenoxyacetate/α-Ketoglutarate Dioxygenase Substrate-Binding Site by Site-Directed Mutagenesis and Mechanism-Based Inactivation†

Julie C. Dunning Hotopp‡,§ and Robert P. Hausinger*,‡,||

*Department of Microbiology and Molecular Genetics and Department of Biochemistry and Molecular Biology, 6193 Biomedical Physical Sciences, Michigan State University, East Lansing, Michigan 48824-4320*

*Received May 1, 2002; Revised Manuscript Received June 6, 2002*

ABSTRACT: TfdA is an Fe(II)- and α-ketoglutarate- (αKG-) dependent dioxygenase that hydroxylates the herbicide 2,4-dichlorophenoxyacetic acid (2,4-D) producing a hemiacetal that spontaneously decomposes to 2,4-dichlorophenol and glyoxylate. On the basis of a recently published TfdA structural model [Elkins et al. (2002) *Biochemistry 41*, 5185−5192], His214, Lys71, Arg278, and the backbone amide of Ser117 are suggested to bind the 2,4-D carboxylate; Lys95 and possibly Lys71 are hypothesized to interact with the 2,4-D ether atom; and Arg274 and Thr141 are suspected to bind αKG. TfdA variants with substitutions at these and other positions were purified and characterized in order to explore the roles of these residues in catalysis. The K71L, K71Q, K95L, K95Q, R274Q, R274L, and R278Q variants exhibited significantly increased 2,4-D $K_m$, αKG $K_m$, and αKG $K_d$ values, consistent with their proposed roles in substrate binding. A protease-sensitive site was successfully eliminated in the R78Q variant, which also exhibited decreased affinity for 2,4-D. In contrast, the Y81F, Y126F, T141V, Y169F, and Y244F variants showed only modest changes in their kinetics. An observed 4-fold lower $K_m$ of the K95L variant compared to wild-type protein with the alternative substrate 2,4-dichlorocinnamic acid provided additional evidence for an interaction between Lys95 and the 2,4-D ether atom. Phenylpropiolic acid was identified as a mechanism-based inactivator of the enzyme [$K_i = 38.1 \pm 6.0$ $\mu$M and $k(\text{inact})_{max} = 2.3 \pm 0.1$ min$^{-1}$]. This acetylenic compound covalently modifies a peptide (166-AEHYALNSR-174) that is predicted to form one side of the substrate-binding pocket. The K95L variant of TfdA was not inactivated by phenylpropiolic acid, providing added support that Lys95 is present at the active site. These results support the identity of suspected substrate-binding residues derived from structural modeling studies and extend our understanding of the oxidative chemistry carried out by TfdA.

α-Ketoglutarate- (αKG-)[1] dependent dioxygenases are mononuclear non-heme Fe(II) enzymes that couple the oxidative decarboxylation of αKG to substrate oxidation (*1*, *2*). Depending on the specific enzyme, the primary substrate may be a protein side chain, a cellular metabolite, or a compound taken up from the environment (*3*). Most commonly, substrate oxidation involves hydroxylation at an unactivated carbon atom, but desaturations, epoxidations, or ring formation or expansion reactions have also been characterized. On the basis of crystal structures of several family members (*4*−*9*) and site-directed mutagenesis studies of the corresponding genes (e.g., ref *10*), Fe(II) is known to be ligated by two histidines and a carboxylic acid-containing side chain, leaving three coordination sites for binding of solvent. Upon binding, αKG displaces two water molecules and chelates the metal via the C-1 carboxylate and C-2 keto group, while the C-5 carboxylate forms a salt bridge with an arginine or lysine side chain. When substrate binds, the final water is displaced, leaving an open coordination site that is available for oxygen activation (*1*, *2*). A "jellyroll" protein architecture serves as the platform for these residues (*4*−*9*), which form a conserved HX(D/E)$X_n$HX$_{(\sim 10)}$(R/K) motif (*10*).

2,4-Dichlorophenoxyacetic acid (2,4-D)/αKG dioxygenase (TfdA) is a representative family member that hydroxylates the herbicide 2,4-D, producing a hemiacetal that spontaneously decomposes to 2,4-dichlorophenol and glyoxylate (Scheme 1). Previous site-directed mutagenesis studies revealed the roles of His114, Asp116, and His263 in binding iron and suggested that His214 functions in 2,4-D binding or catalysis (*10*). Recently, a model of the three-dimensional structure of TfdA (Figure 1) was developed on the basis of the crystal structures of two homologous enzymes, taurine/

† These studies were supported by National Institutes of Health Grant GM063584 and the Michigan State University Agricultural Experiment Station.

* To whom correspondence should be addressed. Tel: 517-355-0780 ext 1610. Fax: 517-353-8957. E-mail: hausinge@msu.edu.

‡ Department of Microbiology and Molecular Genetics.

§ Current address: The Institute for Genomic Research, 9712 Medical Center Drive, Rockville, MD 20850.

|| Department of Biochemistry and Molecular Biology.

[1] Abbreviations: αKG, α-ketoglutarate; CS, clavaminate synthase; DAOCS, deacetoxycephalosporin C synthase; 2,4-D, 2,4-dichlorophenoxyacetic acid; EDTA, ethylenediaminetetraacetic acid; FAB, fast atom bombardment; MALDI, matrix-assisted laser desorption−ionization; PPA, phenylpropiolic acid; TauD, taurine/αKG dioxygenase; TFA, trifluoroacetic acid; TfdA, 2,4-D/αKG dioxygenase; Tris, tris(hydroxymethyl)aminomethane.

10.1021/bi026057a CCC: $22.00 
Published on Web 07/13/2002

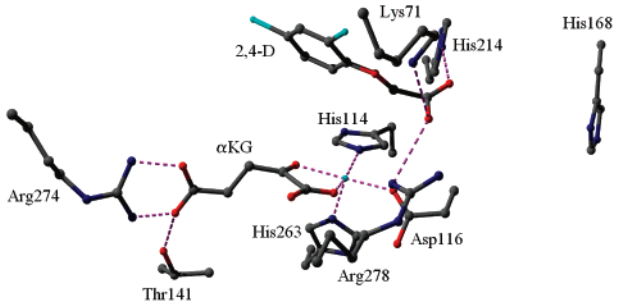


FIGURE 1: Diagram illustrating the predicted positions of active site residues in TfdA. The crystal structures of TauD and CS were previously used to model the homologous protein TfdA (PDB accession number 1GQX) (*9*). The residues believed to be involved in substrate binding, and for which variants were made in these studies, are illustrated. Not shown is Lys95, which is found on a loop that could not be convincingly modeled; however, several possible models positioned this residue where it could interact with the 2,4-D ether atom.

Scheme 1

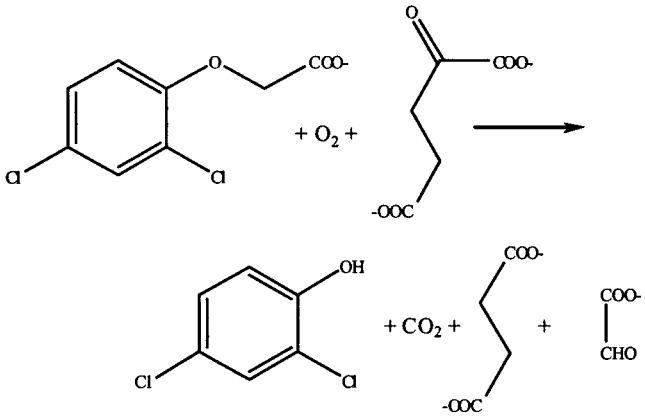


α-ketoglutarate dioxygenase (TauD) (*9*) and clavaminate synthase 1 (CS) (*6*). The TfdA model placed His114, Asp116, and His263 together in a geometry consistent with a metal-binding site, located His214 nearby at the suspected 2,4-D binding site, and revealed that a protease-sensitive site involving Arg78 was located on the surface of the protein. Furthermore, the model newly identified a set of additional residues likely to be involved in 2,4-D and αKG binding.

The studies described here utilize site-directed mutagenesis and mechanism-based inactivation approaches to better define the residues at the substrate-binding site of TfdA. The TfdA model is tested by characterizing selected mutant proteins substituted at the proposed substrate-binding residues. Additional TfdA mutants are characterized in order to assess the effects of altering a residue at the protease-sensitive Arg78 site and to explore the importance of tyrosine residues located near the metal center. Finally, phenylpropiolic acid (PPA) is shown to be a mechanism-based, irreversible inactivator of TfdA that covalently attaches to the protein, thus revealing an additional sequence located at the active site.

## EXPERIMENTAL PROCEDURES

*Site-Directed Mutagenesis.* The amino acid residue numbering scheme used here is based on that derived from the gene sequence rather than that of the purified protein and differs by the addition of the amino-terminal methionine residue compared to that used previously (*10*, *11*). TfdA variants were created using the Stratagene QuikChange mutagenesis system and pUS311 (*12*) as the starting plasmid. This pUC19 derivative contains the *Ralstonia eutropha* JMP134 (pJP4) *tfdA* gene (*13*).

*Protein Purification Methods.* Protein concentrations were determined by using the Bio-Rad assay and bovine serum albumin as the standard. Wild-type and all variant forms of TfdA except Y126F protein were purified from *Escherichia coli* DH5α as previously described (*14*). Y126F TfdA was temperature sensitive so the protein was purified at 4 °C and with alterations to the last two chromatographic steps. Specifically, the active fractions eluting from the DEAE-Sepharose column were pooled, adjusted to 1 M ammonium sulfate, loaded onto a phenyl-Sepharose column (2.5 cm × 19 cm) equilibrated with TE buffer (10 mM Tris, 1 mM EDTA, pH 7.7) containing the same concentration of this salt, and chromatographed with a 400 mL linear gradient from 1 to 0 M ammonium sulfate. The active fractions were dialyzed to remove the ammonium sulfate and then chromatographed on a Q-Sepharose column (2.5 cm × 19 cm) using TE buffer and a 400 mL linear gradient to 200 mM NaCl in TE.

*Kinetic Analyses.* Typical activity measurements used the 4-aminoantipyrene assay (*15*) for detecting 2,4-dichlorophenol. Oxygen consumption and 2,4-dichlorocinnamic acid oxidation were monitored using previously described oxygen electrode and HPLC methods, respectively (*14*). As previously documented (*16*), TfdA activity decreases over time by a combination of irreversible inactivation [possibly associated with an enzymatic self-hydroxylation process (*11*)] and ascorbate-reversible inactivation (presumably due to metal oxidation). For the wild-type enzyme and some of its variants, the inactivation rate is insignificant over the course of a typical assay and linear kinetics were assumed. For several variant proteins, however, the activity was observed to decrease over the assay time course; thus, progress curves were analyzed by fitting the data to eq 1 where $P_t$ is the

$$P_t = V_i(1 - e^{-k(\text{inact})t})k(\text{inact})^{-1} \quad (1)$$

accumulated product at time $t$, $V_i$ is the initial velocity, and $k$(inact) is the inactivation rate constant (*16*). In cases where high concentrations of substrate were found to decrease the $k_{cat}$, the data were analyzed for competitive substrate inhibition (measured as $K_{si}$) by fitting to eq 2. The $K_d$ values

$$k = \frac{k_{cat}[S]}{K_m + [S] + [S]^2/K_{si}} \quad (2)$$

associated with binding of Fe(II) and αKG to TfdA and its variants were measured by using intrinsic tryptophan fluorescence and fitting to eq 3 as previously described (*17*). In

$$\Delta F = \Delta F_{max}\,(K_d + [L_T] + [E_T] - \sqrt{(K_d + [L_T] + [E_T])^2 - 4[L_T][E_T]})/2[E_T] \quad (3)$$

this equation, the observed changes in fluorescence ($\Delta F$) are related to the maximal fluorescence change ($\Delta F_{max}$) extrapolated to infinite concentration of titrant. On the basis of the known total concentrations of enzyme subunit ([$E_T$]) and

ligand ([$L_T$]), the $K_d$ and $\Delta F_{max}$ were calculated. Curve fits were computed using KaleidaGraph for Windows by Abelbeck Software.

*Kinetics of TfdA Inactivation by Phenylpropiolic Acid.* The inactivation of TfdA by PPA was studied in 10 mM imidazole, 1 mM αKG, 5 $\mu$M $(NH_4)_2Fe(SO_4)_2 \cdot 6H_2O$, and 20 $\mu$M ascorbic acid containing varying concentrations of the inactivator at 30 °C. Stock solutions of all reagents were made fresh prior to each set of experiments. Aliquots were withdrawn at the indicated time intervals and diluted 100-fold into fresh assay buffer containing 1 mM 2,4-D, and residual activities were determined as in the standard 4-aminoantipyrene assay procedure. These data were plotted according to log(residual activity) versus time in order to obtain the inactivation rates, *k*(inact), and further analyzed by fitting to the equation:

$$k(\text{inact}) = \frac{k(\text{inact})_{max}[\text{I}]}{K_i + [\text{I}]} \quad (4)$$

where [I] is the inactivator concentration, $k(\text{inact})_{max}$ is the inactivation rate at saturating [I], and $K_i$ is the [I] that gives rise to half-maximal rates of inactivation.

*Large-Scale Inactivation of TfdA by PPA Followed by Alkylation and Protease Digestion.* TfdA (1−5 mg) was inactivated by PPA in 10 mM imidazole buffer (pH 6.8) containing 1 mM αKG, 1 mM PPA, 5 $\mu$M $(NH_4)_2Fe(SO_4)_2 \cdot 6H_2O$, and 20 $\mu$M ascorbic acid at 30 °C. Inactivation was complete by 2 min as confirmed by using the 4-aminoantipyrene assay. PPA-treated protein was dialyzed against water, lyophilized, and redissolved in 6 M guanidine hydrochloride, 100 mM Tris (pH 8), and 10 mM EDTA. Using darkened vials, the sample was degassed, and dithiothreitol was added at 10-fold excess over the cysteines. After 30 min at 50 °C, iodoacetate was added in 2-fold excess to dithiothreitol. The alkylation reaction was quenched with excess $\beta$-mercaptoethanol, and the sample was dialyzed into 50 mM ammonium bicarbonate (pH 7.8). TPCK-treated trypsin (1% w/w, Sigma) was added twice with incubation at 37 °C for 1 h after each addition. Digestion was confirmed by sodium dodecyl sulfate−polyacrylamide gel electrophoresis (*18*) and matrix-assisted laser desorption−ionization (MALDI) mass spectrometry (Michigan State University Mass Spectrometry Facility).

The MALDI mass spectra were measured using a Voyager STR time-of-flight mass spectrometer (Perceptive Biosystems, Framingham, MA) equipped with a nitrogen laser (337 nm, 3 ns pulse). Spectra were measured in the linear mode of operation. The accelerating potential of the Voyager instrument was +25 kV. The MALDI spectra represent the accumulation of 50−100 laser shots, fired at the sample. The sample matrix α-cyano-4-hydroxycinnamic acid was dissolved in water/acetonitrile (1:1 v/v) to give a saturated solution at room temperature. To prepare the sample, 0.5 $\mu$L of the peptide solution (1−10 pmol/$\mu$L of 0.1% trifluoroacetic acid) was added to 0.5 $\mu$L of matrix and applied on a stainless steel target. The solution was left to dry at room temperature, and the sample plate was inserted into the mass spectrometer and analyzed. Time to mass conversion was achieved by internal or external calibration using bradykinin and adrenocorticotropic hormone (18−39).

Table 1: 2,4-D-Related Kinetics of Variant TfdA Proteins[a]

| variant | range ($\mu$M) | $k_{cat}$ ($min^{-1}$) | $K_m$ ($\mu$M) | $k_{cat}/K_m$ ($min^{-1}$ $mM^{-1}$) | $K_{si}$[b] (mM) |
|---|---|---|---|---|---|
| wild type[c] | 5−1000 | 1020 ± 90 | 20.0 ± 5.4 | 51000 | |
| K71L[d,e] | 100−10000 | 256 ± 48 | 370 ± 170 | 692 | 16 ± 11 |
| K71Q[d,e] | 100−10000 | 2093 ± 150 | 1100 ± 300 | 1900 | |
| R78Q | 125−5000 | 452 ± 21 | 1500 ± 200 | 301 | |
| Y81F | 5−1000 | 346 ± 12 | 33.2 ± 3.3 | 10400 | |
| K95L[d,e] | 25−1000 | 893 ± 41 | 78.5 ± 12 | 11400 | |
| K95Q | 10−1000 | 733 ± 22 | 39.5 ± 5.2 | 18600 | |
| Y126F | 5−1000 | 576 ± 26 | 31.9 ± 5.1 | 18100 | |
| T141V | 5−1000 | 707 ± 19 | 21.6 ± 2.2 | 32700 | |
| Y169F | 5−1000 | 444 ± 10 | 42.9 ± 5.1 | 10300 | |
| Y244F | 5−1000 | 512 ± 32 | 30.8 ± 4.0 | 16600 | |
| R274Q[e,f] | 250−10000 | 208 ± 16 | 1600 ± 30 | 131 | 39 ± 18 |
| R274L | 250−10000 | 296 ± 176 | 2500 ± 1300 | 118 | 9.9 ± 7.4 |
| R278Q[e,f] | 250−10000 | 256 ± 17 | 4200 ± 200 | 160 | 11 ± 8 |

[a] The kinetics were linear during the time course of the assay, and 1 mM αKG was utilized, except where noted. [b] Substrate inhibition constant calculated according to eq 2. [c] Previously published (*12*). [d] Values were determined using 10 mM αKG. [e] Reaction progress was nonlinear during the course of the assay, and data were analyzed by using eq 1. [f] Values were determined using 2 mM αKG.

*Separation and Characterization of TfdA Peptides.* The tryptic digests of control and modified proteins were chromatographed on a pep-RPC (HR10/10) (Pharmacia) column by using a linear 200 mL gradient from 0.1% trifluoroacetic acid (TFA) in water to methanol containing 0.1% TFA while monitoring the absorption at 280 nm. All peptides absorbing at this wavelength were characterized by MALDI mass spectrometry (Michigan State University Mass Spectrometry Facility). In addition, the aromatic species uniquely identified in the PPA-treated sample was subjected to fast atom bombardment (FAB) mass spectrometry. FAB mass spectra were obtained using a JEOL HX-110 double-focusing mass spectrometer (JEOL USA, Peabody, MA) operating in the positive ion mode. Ions were produced by bombardment with a beam of Xe atoms (6 keV). The accelerating voltage was 10 kV, and the resolution was set at 1000. The samples were scanned from *m*/*z* 50 to *m*/*z* 1500. Spectra are derived from averaging five to seven scans.

## RESULTS

*Site-Directed Mutagenesis of Proposed 2,4-D Ligands.* R278Q, K71L, K71Q, K95L, and K95Q TfdA variants were purified and characterized to assess the roles of these residues in catalysis and 2,4-D binding. Iron binding to these proteins was not affected on the basis of $K_d$ determinations using previously described (*17*) fluorescence techniques (data not shown). Kinetic analyses revealed only modest changes in $k_{cat}$, with an approximately 2-fold increase in the rate for the K71Q mutant and 4−5-fold decreases for the K71L and R278Q variants (Table 1). The most striking changes observed for these proteins involved $K_m$, ranging from a 2-fold increase in the case of K95Q to a 200-fold increase for R278Q (Table 1). The large increases in $K_m$ result in corresponding decreases in the catalytic efficiency ($k_{cat}/K_m$) of these variants (Table 1). The observed changes in 2,4-D $K_m$ are likely to correlate with the $K_d$ changes; however, the values need not be related. Direct determination of the 2,4-D $K_d$ by the fluorescence quenching approach was not possible because 2,4-D, along with all other TfdA substrates, absorb at the fluorescence excitation wavelength and interfere with

Scheme 2

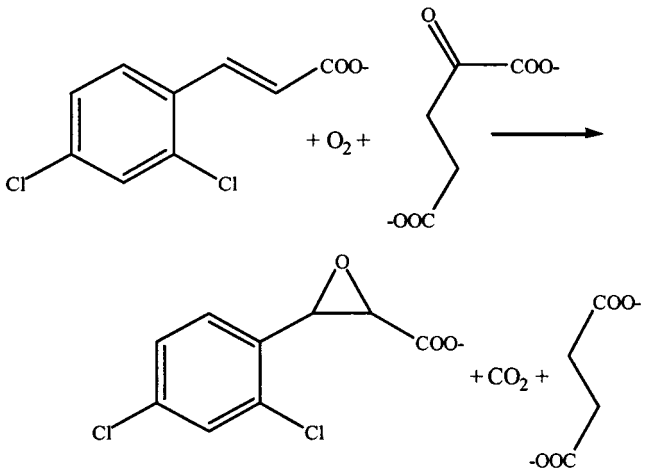


the analysis. Nevertheless, the steady-state kinetic results are consistent with a role for Arg278, Lys71, and perhaps Lys95 in substrate binding.

To further examine the roles of these suspected 2,4-D binding residues, the variant proteins were incubated with the alternative substrate 2,4-dichlorocinnamic acid. This compound resembles 2,4-D but possesses a carbon−carbon double bond in the side chain rather than the ether oxygen. Wild-type TfdA converts 2,4-dichlorocinnamic acid to the epoxide, 2,4-dichlorophenylglycidic acid (Scheme 2), with a $K_m$ of 190 ± 56 $\mu$M and a $k_{cat}$ of 52.5 ± 5.1 min$^{-1}$ (*14*). No detectable epoxidation activity was observed for the K71L, K71Q, and R278Q variants of TfdA in the presence of 1 mM 2,4-dichlorocinnamic acid (higher concentrations could not be tested due to its limited solubility in water). In contrast, both the K95Q and K95L variants were shown to oxidize the aliphatic substrate. Whereas the K95Q variant had an estimated $K_m$ >500 $\mu$M for this compound, K95L TfdA had an approximate 4-fold decrease in the $K_m$ and similar $k_{cat}$ for 2,4-dichlorocinnamic acid ($K_m$ = 56.5 ± 14.0 $\mu$M and $k_{cat}$ = 41.3 ± 3.2 min$^{-1}$) when compared to wild-type enzyme. These results are consistent with participation of Lys95 in 2,4-D binding but not in 2,4-dichlorocinnamic acid binding.

*Site-Directed Mutagenesis of Proposed αKG Ligands.* T141V, R274L, and R274Q variants of TfdA were purified and characterized to assess the roles of these residues in catalysis and αKG binding (Tables 1 and 2). None of the variants exhibited significant differences in iron $K_d$ (not shown), and the substitutions had only modest effects on $k_{cat}$. T141V also had no significant change in its αKG $K_m$, αKG $K_d$, or 2,4-D $K_m$, suggesting that it has at most a minor role in binding to αKG. In contrast, R274L and R274Q were found to have ~1000-fold increases in the αKG $K_m$ and $K_d$ (Table 2), thus confirming the critical role for Arg274 at the active site. To examine whether the reduced activity of R274Q TfdA could be overcome by use of a different cosubstrate, several alternative α-keto acids were examined. The enzyme used α-ketocaproate and α-ketoisovalerate with $K_m$ values of 1.7 ± 0.5 mM and 0.70 ± 0.09 mM and $k_{cat}$ values of 365 ± 31 min$^{-1}$ and 22.4 ± 2.8 min$^{-1}$, respectively.

*Arg78.* To eliminate a protease-sensitive site in TfdA (*12*), the R78Q variant was constructed and characterized. In contrast to the situation for wild-type protein, no significant proteolysis product was observed. Although the TfdA model suggests that Arg78 is not located near the active site, the R78Q variant exhibited a nearly 100-fold increase in the 2,4-D $K_m$. This variant was unaffected in the iron $K_d$ and, unlike variants of the active site 2,4-D binding residues, did not have an increase in the αKG $K_d$ or αKG $K_m$. This lack of effect on αKG binding is consistent with the residue not being in the active site.

*Site-Directed Mutagenesis of Tyrosines Located near the Active Site*. Tyrosine mutants of TfdA were of interest because a tyrosine radical has been detected in TauD (a 30% identical protein) and considered as a possible catalytically relevant intermediate (M. J. Ryle, A. Liu, R. B. Muthukumaran, R. Y. N. Ho, J. McCracken, L. Que, Jr., and R. P. Hausinger, unpublished observations). To assess the importance of the four TfdA tyrosines predicted to lie closest to the active site (Tyr81, Tyr126, Tyr169, and Tyr244), each was individually substituted with phenylalanine, and the variant enzymes were characterized. All four variants were only slightly affected when compared to wild-type enzyme in terms of iron $K_d$, αKG $K_d$, αKG $K_m$, and 2,4-D $K_m$ (Tables 1 and 2), suggesting that these tyrosines are not involved in catalysis or substrate binding. The Y81F, Y168F, and Y244F proteins were purified by previously described procedures, but Y126F TfdA had the unique characteristic of rapidly precipitating unless maintained at low temperature. This lability was not evident during the typical time course of the assay but was observed during the initial purification steps at room temperature. The lack of temperature sensitivity during catalysis may imply that the presence of one or more of the substrates stabilizes the protein during activity measurements.

*Inactivation of TfdA by PPA.* As an alternative approach to examine residues at the substrate-binding site, PPA, an acetylenic analogue of 2,4-D, was examined as a possible mechanism-based inactivator. PPA appeared to strongly inhibit or inactivate the enzyme on the basis of the absence of oxygen consumption after addition of 2,4-D to protein previously incubated with iron, αKG, ascorbate, and this compound. Kinetic analysis of enzyme inactivation revealed a first-order loss of activity (Figure 2, panel A) that was dependent on the concentration of PPA and required αKG and ferrous ions. Consistent with binding of the inactivator to the active site, high concentrations of 2,4-D protected the enzyme against inactivation. Saturation kinetics were observed for the loss of activity, allowing the calculation of $K_i$ = 38.1 ± 6.0 $\mu$M and $k(\text{inact})_{max}$ = 2.3 ± 0.1 min$^{-1}$ (Figure 2, panel B). Inactivation of TfdA by PPA was not reversible by dialysis against 10 mM imidazole (pH 6.8) for 72 h, consistent with it being an irreversible, mechanism-based inactivator.

In contrast to wild-type TfdA that was inactivated within 1 min, no inactivation of the K95L variant was observed for up to 4 min at 1 mM PPA. The K71L, K71Q, and R278Q variants were not examined by this approach since they have significantly increased 2,4-D $K_m$ values and would likely bind the inactivator poorly. As a control, the Y81F variant was found to be inactivated by PPA at the same rate as wild-type enzyme (data not shown). The lack of inactivation in the K95L mutant was not due to a lack of binding since PPA is a competitive inhibitor with respect to 2,4-D with a $K_i \approx 60$ $\mu$M (Figure 3).

Table 2: αKG-Related Kinetics of Variant TfdA Proteins[a]

| variant | range (μM) | $k_{cat}$ ($min^{-1}$) | $K_m$ (μM) | $k_{cat}/K_m$ ($min^{-1}$ $mM^{-1}$) | $K_d$ (μM) | $K_{si}$[b] (mM) |
|---|---|---|---|---|---|---|
| wild type | | 643 ± 44[c] | 3.2 ± 0.6[c] | 201000[c] | 3.4 ± 0.4 | |
| K71L[d,e] | 2500−$10^6$ | 112 ± 10 | 11700 ± 3300 | 9.6 | 2100 ± 400 | |
| K71Q[d,e] | 2500−$10^6$ | >1900 | >20000 | | 4800 ± 300 | |
| R78Q | 5−1000 | 403 ± 45 | <40 | >10100 | 9.9 ± 0.7 | |
| Y81F | 5−1000 | 285 ± 21 | <10 | >28500 | 8.9 ± 0.7 | |
| K95L[d] | 5−1000 | 461 ± 51 | <35 | >13200 | 10.0 ± 1.1 | |
| K95Q | 5−1000 | 301 ± 5 | <10 | >20100 | 14.9 ± 2.6 | |
| Y126F | 5−1000 | 435 ± 3 | <20 | >21800 | 14.8 ± 1.0 | |
| T141V | 5−1000 | 560 ± 48 | <20 | >28000 | 10.9 ± 1.2 | |
| Y169F | 5−1000 | 454 ± 14 | <10 | >45000 | 11.1 ± 2.2 | |
| Y244F | 5−1000 | 512 ± 32 | <10 | >51200 | 16.6 ± 3.7 | |
| R274Q[d,f] | 500−$10^6$ | 263 ± 72 | 8200 ± 3900 | 32 | 2300 ± 200 | 44 ± 24 |
| R274L | 250−$10^6$ | 271 ± 68 | 4800 ± 2700 | 56 | 9000 ± 600 | 116 ± 92 |
| R278Q[d,f] | 500−$10^6$ | 224 ± 12 | 4100 ± 500 | 53 | 1350 ± 50 | 133 ± 24 |

[a] The kinetics were linear during the time course of the assay and utilized 1 mM 2,4-D, except where noted. [b] Substrate inhibition constant calculated according to eq 2. [c] Data from Fukumori et al. (*12*). [d] Reaction progress was nonlinear during the course of the assay, and data were analyzed by using eq 1. [e] Determined using 10 mM 2,4-D. [f] Determined using 2 mM 2,4-D.

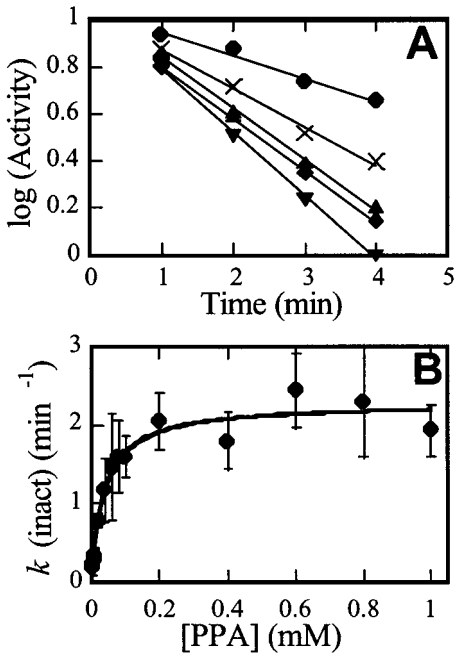


FIGURE 2: TfdA inactivation kinetics in the presence of PPA. (A) First-order loss of activity over time for 2 μM (●), 4 μM (×), 6 μM (◆), 8 μM (▲), and 10 μM (▼) PPA. (B) Inactivation rates versus the concentration of PPA, fit to eq 4.

PPA-treated and untreated samples of wild-type TfdA were digested with trypsin and compared by using MALDI mass spectrometry and reverse-phase chromatography. No differences were observed between the direct MALDI analyses of digestions of modified and unmodified proteins (data not shown), even though 92% of the peptides with molecular masses between 1100 and 2600 Da were able to be identified. In an extension of these studies, the tryptic digests were subjected to reverse-phase column chromatography while monitoring the absorbance at 280 nm (allowing detection of peptides containing Trp, Tyr, and the PPA aromatic ring). Comparison of the chromatography profiles revealed a novel peak in the PPA-treated sample (labeled * in Figure 4, bottom) compared to the profile of untreated sample (Figure 4, top). In addition, a diminution in intensity and change in shape typically was observed for peak 1 of the PPA-treated sample (changes in this feature were more apparent in other preparations). Each of the 280 nm absorbing peaks was collected from the chromatography of the modified protein and analyzed by MALDI mass spectrometry (Table 3). The peptide molecular weights revealed by the MALDI analyses indicated that peak 1 contained two Tyr-containing peptides and showed that all four Trp and all seven Tyr in TfdA were accounted for. Notably, the purified peptide containing Lys95 (peak 5) gave a very weak MALDI signal, and this peak suppression was consistent with the inability to detect this peptide during MALDI analysis of the whole digest peptide mixture. The sample in the fraction corresponding to the novel 280 nm absorbing peak also exhibited MALDI suppression problems, so that no novel mass was observed in the PPA-treated protein compared to the nontreated control. By contrast, FAB mass spectrometric analysis consistently revealed masses at 1177 and 1222 Da in both positive and negative ion modes. A mass of 1222 Da is consistent with the addition of phenylpropiolic acid (146 Da) and oxygen, and loss of a hydrogen atom, to the peptide corresponding to 166-AEHYALNSR-174 (1061 Da). A mass of 1177 could reasonably result from the decarboxylation of this same modified peptide (α-keto acids are known to be readily decarboxylated). Notably, the nonmodified form of this peptide elutes in peak 1, which is altered in appearance between the treated and nontreated samples. The small difference in intensities of peak 1 in the two samples, accounting for less than 20% absorption loss, suggests that modification of this peptide is substoichiometric. N-Terminal sequencing of the fraction containing the novel peak only revealed the sequence of the contaminating peptide from peak 5, suggesting that the modified peptide is blocked close to the N-terminus.

## DISCUSSION

On the basis of TfdA structural modeling studies, interactions with the 2,4-D carboxylic acid were suggested to involve Arg278, Lys71, His214 (Figure 1), and the backbone amide of Ser117 (not shown) (*9*). The model also indicated that a loop comprising residues 86−111 made up one face of the 2,4-D binding pocket; however, a consensus structure for this region could not be obtained, and these 25 residues were omitted from the final model. Notably, several possible structures for this loop placed Lys95 where it could assist

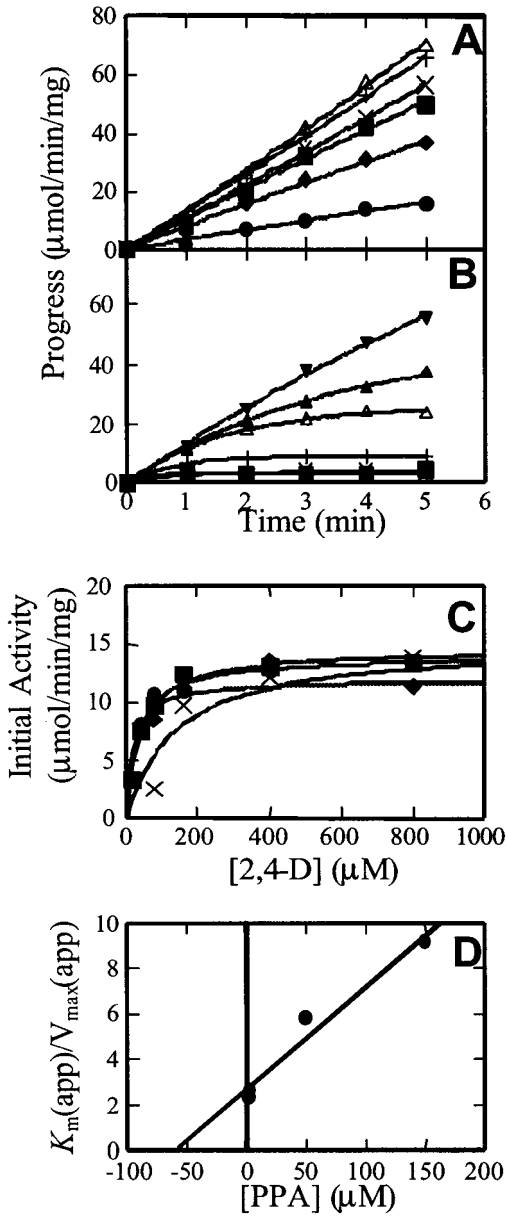


FIGURE 3: PPA competitive inhibition kinetics for K95L TfdA. Panels A and B depict progress curves of the K95L variant enzyme incubated with 2.5 $\mu$M and 150 $\mu$M PPA, respectively, with varying 2,4-D concentrations [16 $\mu$M (●), 40 $\mu$M (◆), 80 $\mu$M (■), 160 $\mu$M (×), 400 $\mu$M (+), 800 $\mu$M (△), 1600 $\mu$M (▲), and 4000 $\mu$M (▼)]. (C) The initial reaction velocities of the above and additional progress curves [utilizing 1.25 $\mu$M (●), 2.5 $\mu$M (■), 50 $\mu$M (◆), and 150 $\mu$M (×) PPA] were plotted versus the concentration of 2,4-D. (D) The $K_m$ of PPA for the K95L protein was deduced by replotting the apparent $K_m/V_{max}$ as a function of PPA concentration.

in binding 2,4-D via interactions with the carboxylate or the ether moiety. In an effort to test this model, we used a site-directed mutagenesis approach. Previous studies had provided evidence for the participation of His214 in binding 2,4-D (*10*), supporting at least that portion of the model. The current investigation focused on Arg278, Lys71, and Lys95 variants of TfdA and demonstrated that proteins altered at each of these positions exhibit decreased affinity for 2,4-D. Additional studies with a Lys95 variant and the alternative substrate 2,4-dichlorocinnamic acid supported the participation of this residue in binding 2,4-D. Whereas the K71L, K71Q, and R278Q variants of TfdA did not metabolize this substrate, presumably due to large increases in 2,4-dichlorocinnamic acid $K_m$ similar to their increased 2,4-D $K_m$, the K95L variant exhibited higher catalytic efficiency for the aliphatic substrate than found with wild-type enzyme. These results imply that changing the basic lysine to the more hydrophobic leucine at the active site enhances the substrate preference for the more aliphatic side chain of 2,4-dichlorocinnamic acid, consistent with Lys95 having a role in binding the ether of 2,4-D. We conclude that Lys71 and Arg278 have important roles in binding the carboxylate of 2,4-D and that Lys95 interacts with the 2,4-D ether oxygen, as predicted by the TfdA structural model. Residues homologous to Arg278 are conserved in several other αKG-dependent dioxygenases (see sequence comparison in ref *9*), whereas Lys71 and Lys95 are not conserved. Given the diversity of substrate structures used by these enzymes, the lack of substrate-binding site conservation is not unexpected.

Many of the αKG-dependent dioxygenases have a conserved arginine and threonine/serine motif, the residues of which are shown or hypothesized to interact with the C-5 carboxylate of αKG (*5*−*10*). In TfdA, this motif is comprised of Arg274 and Thr141 (*10*) as predicted by our computer-

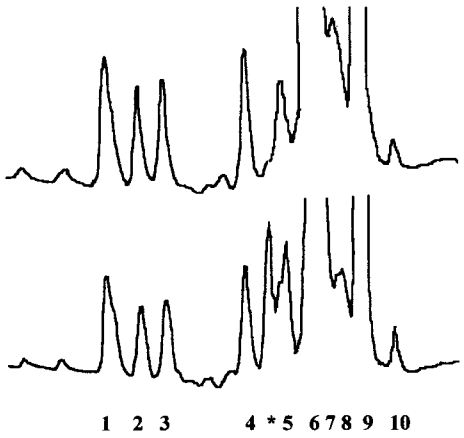


FIGURE 4: Peptide purification and identification. Tryptic digests of (top) untreated and (bottom) PPA-treated TfdA were chromatographed on a reverse-phase column while the absorption was monitored at 280 nm. The asterisk indicates a peak observed only in the treated sample.

Table 3: MALDI Mass Spectrometric Analysis of PPA-Treated TfdA Tryptic Peptides[a]

| peak no. | molecular weight | sequence |
|---|---|---|
| 1 | 1061.3 | 166-AEH**Y**ALNSR-174 |
| | 881.2 | 267-R**Y**DISAR-273 and/or 268-**Y**DISARR-274 |
| 2 | 714.0 | 241-EFV**Y**R-245 |
| 3 | 877.2 | 148-AA**Y**DALPR-155 |
| 4 | 1515.1 | 175-FLLGDTD**Y**SEAQR-187 |
| 5 | 1595.1 | 81-**Y**AELADISNVSLDGK-95 |
| 6 | 1394.4 | 188-NAMPPVN**W**PLVR-199 |
| 7 | 2589.8 | 103-EVVGNFANQL**W**HSDSSFQQPAAR-125 |
| 8 | 2420.2 | 126-**Y**SMLSAVVVPPSGGDTEFCDMR-147 |
| 9 | 1505.2 | 248-**W**NVGDLVM**W**DNR-259 |
| 10 | 2234.0 | unidentified |
| | 1525.1 | unidentified |

[a] Each of the 280 nm absorbing peaks collected from the chromatograph of Figure 4 for PPA-modified protein was examined by MALDI mass spectrometry. The molecular masses of the major MALDI species are indicated, along with the sequences corresponding to these masses. Aromatic residues are highlighted in bold.

generated structural model (*9*) (Figure 1). Mutagenesis studies were carried out to test whether these residues are critical to αKG binding. Arg274 was shown to play a substantial role in binding αKG, whereas Thr141 has only a minor, if any, role in interacting with αKG. Codons encoding the analogous threonine residue have not been mutated in other family subgroup members; however, the corresponding arginine residues have been substituted in several related enzymes. For example, conversion of this arginine in deacetoxycephalosporin C synthase (DAOCS, another αKG-dependent dioxygenase) to a glutamine was reported not to affect the $K_m$ of its primary substrate (*19*). The loss of activity arising from conversion of the corresponding arginine to glutamine in DAOCS (and phytanoyl-CoA hydroxylase, another family member) was found to be reversed by using longer chain length α-keto acids, a phenomenon termed cosubstrate rescue (*19*, *20*). In particular, α-ketocaproate and α-ketoisovalerate restored activity to greater than 100% of the αKG-dependent wild-type activity in the R258Q mutant of DAOCS. Cosubstrate rescue was not observed with the R274Q variant of TfdA using either α-ketocaproate or α-ketoisovalerate. The reasons for the differences in behavior of the arginine mutants in TfdA versus DAOCS or phytanoyl-CoA hydroxylase are not clear.

In addition to mutating codons encoding the residues hypothesized from the model to be involved in substrate binding, Arg78 was converted to a glutamine in order to eliminate a protease-sensitive site in TfdA (*12*) and the requirement for several tyrosine residues was examined. Our successful removal of the protease-sensitive site might be beneficial in future crystallography efforts, since preliminary attempts to crystallize TfdA have been stymied, in part, by the heterogeneity of the sample due to the presence of the proteolysis product. Although this arginine residue is predicted to lie on the protein surface distant from the active site, a significant increase in 2,4-D $K_m$ was observed for the R78Q variant. A hypothetical role of Arg78 is to act as a gate for 2,4-D entry into the active site. This role also has been hypothesized for His217, since the alanine variant (H217A) of this residue has an increased 2,4-D $K_m$ but is not in the active site (*10*). Possibly related to these findings, the crystal structure of the αKG-dependent dioxygenase anthocyanidin synthase reveals two bound substrate molecules with one binding site proposed to assist in transfer of substrate to the active site (*8*). Our mutagenesis studies involving four tyrosine residues located near the TfdA active site rule out any essential role for these residues.

Lysines and arginines are expected to have multiple hydrogen-bonding partners because of their large size and positively charged side chains. Substitution of these residues could reasonably have long-range effects. One such effect observed here is the significantly increased αKG $K_m$ and αKG $K_d$ of the 2,4-D-binding site mutants (Table 2), possibly resulting from repositioning of various active site residues, shifting of the protein backbone, and/or disruption of secondary structure elements. Complementary results were observed with the R274L and R274Q mutations involving the αKG-binding site; i.e., the 2,4-D $K_m$ increased ~100-fold (Table 1). Such interactions between two substrate-binding sites are not unexpected but have not been documented in prior mutagenesis studies within this enzyme family.

Scheme 3: Theoretical Mechanism of TfdA Inactivation by PPA, Based on the Inactivation Mechanism Determined for the Thymine Hydroxylation Interaction with an Acetylenic Substrate Analogue[a]

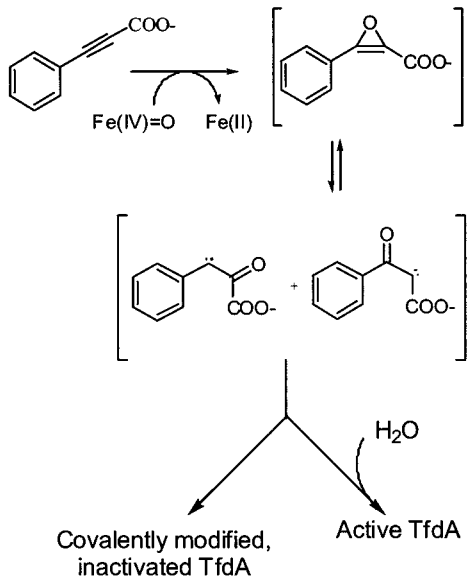


[a] References *21*−*23*.

PPA was demonstrated to be a mechanism-based inactivator of TfdA. A reasonable mechanism for how PPA reacts with TfdA is illustrated in Scheme 3. Initial oxidation of PPA by TfdA likely produces a highly reactive oxirene intermediate that rearranges to form either of two carbene intermediates. Analogous oxidative chemistry was established for thymine hydroxylase, an αKG-dependent dioxygenase that is inactivated upon treatment with an acetylenic analogue of thymine (*21*−*23*). In addition, cytochrome P450 enzymes are known to catalyze this type of reaction with acetylenic compounds (*24*). Low-energy interconversions between oxirene and carbenes on adjacent carbon atoms are well documented (*25*, *26*). Since carbenes are known to be able to react with amino acid side chains, a covalent linkage could reasonably form between oxidized PPA and a TfdA active site residue. Alternatively, carbenes may react with solvent to spare the enzyme and release an aromatic product. To explore this model further, two approaches were used: PPA-dependent inactivation kinetics were analyzed using the previously prepared K95L variant and peptide studies were carried out on PPA-inactivated TfdA.

Modeling and site-directed mutagenesis studies indicate that Lys95 is likely to be positioned near the 2,4-D ether oxygen and thus may lie close to the suspected oxirene intermediate formed from PPA acid. The K95L variant of TfdA was found to be resistant to inactivation by PPA. A reasonable explanation for the observed lack of inactivation is that the carbene intermediate formed by the enzyme reacts with water (Scheme 3), as previously described for inactivation of thymine hydroxylase by an acetylenic substrate analogue (*21*−*23*). For example, replacement of Lys95 by Leu may result in greater solvent access to the active site. Arguing against this scenario, however, K95L TfdA did not release detectable quantities of a new aromatic product arising from PPA when analyzed by HPLC, and turnover of PPA by the variant enzyme was indiscernible on the basis of oxygen consumption. While the mechanism by which

K95L TfdA resists inactivation by PPA remains unclear, these results are consistent with the placement of Lys95 at the active site.

MALDI mass spectrometric studies of tryptic peptides derived from PPA-treated wild-type TfdA are consistent with a covalent linkage formed between PPA and the 166-AEHYALNSR-174 peptide. Portions of this peptide are predicted to lie close to the 2,4-D binding site (e.g., the Ser173 side chain hydroxyl is located only 5.4 Å from the 2,4-D carboxyl group) according to the TfdA model. Substitution of Tyr169 by Phe produced no effect on activity or binding of 2,4-D or αKG (Tables 1 and 2). In contrast, previous studies analyzing the H168A TfdA variant (as a maltose binding protein fusion) resulted in an inactive enzyme (*10*). The mutagenesis and PPA-dependent inactivation results are consistent with the indicated peptide being present at the active site with His168 playing a role in catalysis. Of interest, a basic residue is conserved at this position in all sequenced 2,4-D/αKG dioxygenases (*10*). These PPA reactivity studies extend our understanding of the range of chemistry available to TfdA by indicating the enzyme's ability to oxidize an acetylenic compound.

## ACKNOWLEDGMENT

We thank Rhonda Husain and Beverly Chamberlain for discussions about interpreting mass spectrometric data and members of the Hausinger laboratory for useful comments.

## REFERENCES

1. Ryle, M. J., and Hausinger, R. P. (2002) Non-heme iron oxygenases, *Curr. Opin. Chem. Biol. 6*, 193−201.
2. Solomon, E. I., Brunold, T. C., Davis, M. I., Kemsley, J. N., Lee, S.-K., Lehnert, N., Neese, F., Skulan, A. J., Yang, Y.-S., and Zhou, J. (2000) Geometric and electronic structure/function correlations in non-heme iron enzymes, *Chem. Rev. 100*, 235−349.
3. Prescott, A. G., and Lloyd, M. D. (2000) The iron(II) and 2-oxoacid-dependent dioxygenases and their role in metabolism, *Nat. Prod. Rep. 17*, 367−383.
4. Roach, P. L., Clifton, I. J., Fülöp, V., Harlos, K., Barton, G. J., Hajdu, J., Andersson, K., Schofield, C. J., and Baldwin, J. E. (1995) Crystal structure of isopenicillin *N* synthase is the first from a new structural family of enzymes, *Nature 375*, 700−704.
5. Valegård, K., Terwisscha van Scheltinga, A. C., Lloyd, M. D., Hara, T., Ramaswamy, S., Perrakis, A., Thompson, A., Lee, W.-J., Baldwin, J. E., Schofield, C. J., Hajdu, J., and Andersson, I. (1998) Structure of a cephalosporin synthase, *Nature 394*, 805−809.
6. Zhang, Z., Ren, J., Stammers, D. K., Baldwin, J. E., Harlos, K., and Schofield, C. J. (2000) Structural origins of the selectivity of the trifunctional oxygenase clavaminic acid synthase, *Nat. Struct. Biol. 7*, 127−133.
7. Clifton, I. J., Hsueh, L.-C., Baldwin, J. E., Harlos, K., and Schofield, C. J. (2001) Structure of proline 3-hydroxylase. Evolution of the family of 2-oxoglutarate dependent dioxygenases, *Eur. J. Biochem. 268*, 6625−6636.
8. Wilmouth, R. C., Turnbull, J. J., Welford, R. W. D., Clifton, I. J., Prescott, A. G., and Schofield, C. J. (2002) Structure and mechanism of anthocyanidin synthase from *Arabidopsis thaliana*, *Structure 10*, 93−103.
9. Elkins, J. M., Ryle, M. J., Clifton, I. J., Dunning Hotopp, J. C., Lloyd, J. S., Burzlaff, N. I., Baldwin, J. E., Hausinger, R. P., and Roach, P. L. (2002) X-ray crystal structure of *Escherichia coli* taurine/α-ketoglutarate dioxygenase complexed to ferrous iron and substrates, *Biochemistry 41*, 5185−5192.
10. Hogan, D. A., Smith, S. R., Saari, E. A., McCracken, J., and Hausinger, R. P. (2000) Site-directed mutagenesis of 2,4-dichlorophenoxyacetic acid/α-ketoglutarate dioxygenase. Identification of residues involved in metallocenter formation and substrate binding, *J. Biol. Chem. 275*, 12400−12409.
11. Liu, A., Ho, R. Y. N., Que, L., Jr., Ryle, M. J., Phinney, B. S., and Hausinger, R. P. (2001) Alternative reactivity of an α-ketoglutarate-dependent iron(II) oxygenase: enzyme self-hydroxylation, *J. Am. Chem. Soc. 123*, 5126−5127.
12. Fukumori, F., and Hausinger, R. P. (1993) Purification and characterization of 2,4-dichlorophenoxyacetate/α-ketoglutarate dioxygenase, *J. Biol. Chem. 268*, 24311−24317.
13. Streber, W. R., Timmis, K. N., and Zenk, M. H. (1987) Analysis, cloning, and high level expression of 2,4-dichlorophenoxyacetate monooxygenase gene *tfdA* of *Alcaligenes eutrophus* JPM134, *J. Bacteriol. 169*, 2950−2955.
14. Dunning Hotopp, J. C., and Hausinger, R. P. (2001) Alternative substrates for 2,4-dichlorophenoxyacetate/α-ketoglutarate dioxygenase, *J. Mol. Catal. B: Enzym. 15*, 155−162.
15. Fukumori, F., and Hausinger, R. P. (1993) *Alcaligenes eutrophus* JMP134 "2,4-dichlorophenoxyacetate monooxygenase" is an α-ketoglutarate-dependent dioxygenase, *J. Bacteriol. 175*, 2083−2086.
16. Saari, R. E., and Hausinger, R. P. (1998) Ascorbic acid-dependent turnover and reactivation of 2,4-dichlorophenoxyacetic acid/α-ketoglutarate dioxygenase using thiophenoxyacetic acid, *Biochemistry 37*, 3035−3042.
17. Dunning Hotopp, J. C., Auchtung, T. A., Hogan, D. A., and Hausinger, R. P. (2002) Intrinsic tryptophan fluorescence as a probe of metal and α-ketoglutarate binding to TfdA, a mononuclear non-heme iron dioxygenase, *J. Inorg. Biochem.* (in press).
18. Laemmli, U. K. (1970) Cleavage of structural proteins during the assembly of the head of bacteriophage T4, *Nature 227*, 680−685.
19. Lee, H.-J., Lloyd, M. D., Clifton, I. J., Harlos, K., Dubus, A., Baldwin, J., E., Frere, J.-M., and Schofield, C. J. (2001) Alteration of the cosubstrate selectivity of deacetoxycephalosporin C synthase. The role of arginine 258, *J. Biol. Chem. 276*, 18290−18295.
20. Mukherji, M., Chien, W., Kershaw, N. J., Clifton, I. J., Schofield, C. J., Wierzbicki, A. S., and Lloyd, M. D. (2001) Structure−function analysis of phytanoyl-CoA 2-hydroxylase mutations causing Refsum's disease, *Hum. Mol. Genet. 10*, 1971−1982.
21. Lai, M.-T., Wu, W., and Stubbe, J. (1995) Characterization of a novel, stable norcaradiene adduct resulting from the inactivation of thymine hydroxylase by 5-ethynyluracil, *J. Am. Chem. Soc. 117*, 5023−5030.
22. Thornburg, L. D., and Stubbe, J. (1989) Mechanism-based inhibition of thymine hydroxylase, *J. Am. Chem. Soc. 111*, 7632−7633.
23. Thornburg, L. D., and Stubbe, J. (1993) Mechanism-based inactivation of thymine hydroxylase, an α-ketoglutarate-dependent dioxygenase, by 5-ethynyluracil, *Biochemistry 32*, 14034−14042.
24. Chen, H., Shockcor, J., Chen, W., Espina, R., Gan, L.-S., and Mutlib, A. E. (2002) Delineating novel metabolic pathways of DPC 963, a nonnucleoside reverse transcriptase inhibitor, in rats, characterization of glutathione conjugates of postulated oxirene and benzoquinone imine intermediates by LC/MS and LC/NMR, *Chem. Res. Toxicol. 15*, 388−399.
25. Lewars, E. (2002) The $C_2F_2O$ potential energy surface: a computational study, *J. Mol. Struct. (THEOCHEM) 579*, 155−167.
26. Zhu, Z., Bally, T., Stracener, L. L., and McMahon, R. J. (1999) Reversible interconversion between singlet and triplet 2-naphthyl(carbomethoxy)carbene, *J. Am. Chem. Soc. 121*, 2863−2874.

BI026057A